

SwiftSpatial: Spatial Joins on Modern Hardware

Wenqi Jiang
Systems Group
Department of Computer Science
ETH Zurich
Zurich, Switzerland

Martin Parvanov
Systems Group
Department of Computer Science
ETH Zurich
Zurich, Switzerland

Gustavo Alonso
Systems Group
Department of Computer Science
ETH Zurich
Zurich, Switzerland

ABSTRACT

Spatial joins are among the most time-consuming queries in spatial data management systems. In this paper, we propose *SwiftSpatial*, a specialized accelerator architecture tailored for spatial joins. SwiftSpatial contains multiple high-performance join units with innovative hybrid parallelism, several efficient memory management units, and an integrated on-chip join scheduler. We prototype SwiftSpatial on an FPGA and incorporate the R-tree synchronous traversal algorithm as the control flow. Benchmarked against various CPU and GPU-based spatial data processing systems, SwiftSpatial demonstrates a latency reduction of up to $5.36\times$ relative to the best-performing baseline, while requiring $6.16\times$ less power. The remarkable performance and energy efficiency of SwiftSpatial lay a solid foundation for its future integration into spatial data management systems, both in data centers and at the edge.

PVLDB Reference Format:

Wenqi Jiang, Martin Parvanov, and Gustavo Alonso. SwiftSpatial: Spatial Joins on Modern Hardware. PVLDB, 14(1): XXX-XXX, 2020. doi:XX.XX/XXX.XX

PVLDB Artifact Availability:

The source code, data, and/or other artifacts have been made available at <https://anonymous.4open.science/r/spatial-join-accelerator-F328>.

1 INTRODUCTION

Spatial data processing is the backbone of geographic information systems (GIS) [42, 54], location-based services [78], computer-aided design [37], and scientific simulations [47, 67]. Spatial joins, where two sets of spatial objects are joined based on their spatial relationships, are among the most time-consuming spatial queries even when executed on multi-core CPUs or a cluster of servers [5, 18, 50], thus worth further performance optimizations. For instance, a 2013 study on spatial big data frameworks [5] reported that joining two indexed datasets, totaling fewer than 100 million records, required 10 minutes (32 CPU hours) when executed on eight servers equipped with 192 cores and 1TB of memory in total. After decades of extensive research on efficient indexes and algorithms for spatial joins, further performance gains have become increasingly difficult given a certain computational budget. This prompts the question: *is it possible to improve spatial join performance without demanding more resources such as CPU cores or memory capacity?*

This work is licensed under the Creative Commons BY-NC-ND 4.0 International License. Visit <https://creativecommons.org/licenses/by-nc-nd/4.0/> to view a copy of this license. For any use beyond those covered by this license, obtain permission by emailing info@vldb.org. Copyright is held by the owner/author(s). Publication rights licensed to the VLDB Endowment.

Proceedings of the VLDB Endowment, Vol. 14, No. 1 ISSN 2150-8097. doi:XX.XX/XXX.XX

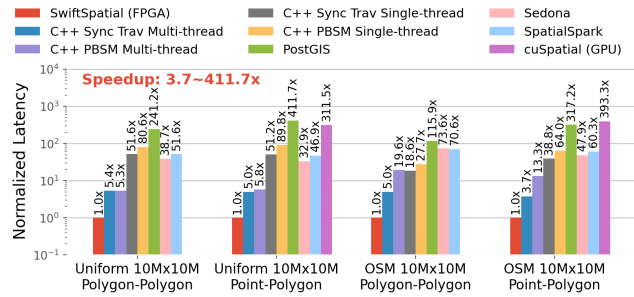


Figure 1: SwiftSpatial achieves up to two orders of magnitude speedup over various CPU and GPU-based systems.

In this paper, we approach spatial join from a hardware acceleration standpoint. To this end, we summarize repetitive patterns observed in efficient spatial join algorithms as follows. During the preprocessing phase, both input datasets are decomposed into small tiles. For example, the datasets can be partitioned using a simple grid (e.g., in PBSM [51, 68]) or indexed by a tree (e.g., R-trees [27, 47, 57]). After preprocessing the datasets, the join process begins, which comprises two primary components. Firstly, a control flow identifies tile pairs from both datasets that could potentially produce results. For example, when both datasets are partitioned using a grid, the control flow selects identical tiles from both datasets; for datasets indexed by R-trees, synchronous traversal [8] is adopted to navigate both trees to identify intersected tile pairs. Secondly, for each candidate tile pair, all objects in the tiles are evaluated based on the predicate to produce results or intermediate outcomes.

Based on these observations, an efficient accelerator for spatial joins should adhere to three key criteria. Firstly, joining each tile pair should be rapid. Secondly, instantiating multiple join units is essential for parallelizing the join across tile pairs. Lastly, the control overhead of coordinating these join units should be minimal, such that the join can be executed efficiently even when dealing with complex control flow such as R-tree synchronous traversal.

We propose *SwiftSpatial*, an in-memory spatial join accelerator whose architecture is tailored to fulfill the three aforementioned criteria, thus achieving high performance and requiring low power supply simultaneously. First, each SwiftSpatial join unit is optimized to achieve minimal latency when joining two spatial object tiles. Its superior performance stems from the innovative architecture that employs hybrid parallelism: (a) operator parallelism for fast predicate evaluation involving multiple object boundary comparisons and (b) pipeline parallelism between input ingestion, join predicate evaluation, and result production for qualifying object pairs. The hybrid parallelism allows a join unit to process an object pair every clock cycle, leading to high and predictable tile-level join performance. Second, multiple join units can be instantiated to

parallelize joins across different tiles. Third, SwiftSpatial incorporates an on-chip scheduler to orchestrate these join units, passing control signals directly to the join units, thus supporting complex control flow with minimal performance overhead. Apart from the join and control units, SwiftSpatial features specialized memory management units to further improve join performance. By directly managing the physical address space, the memory management units (a) optimize memory access patterns through memory request batching and memory address rewriting, and (b) avoid the overhead associated with page table management and dynamic memory allocation prevalent in software systems.

We prototype SwiftSpatial on an FPGA and adopt the widely-used R-tree synchronous traversal algorithm as the control flow. We choose FPGA as the hardware platform for two reasons: (a) it allows us to build and evaluate the accelerator without relying on hardware simulations or the costly and inflexible ASIC tape-out, and (b) the growing adoption of FPGAs in data centers, as seen in industry giants like Microsoft [22], Amazon [2], Alibaba [39], facilitates the integration of SwiftSpatial into spatial data management systems. Our choice of the R-tree synchronous traversal is rooted in three considerations. First, it is the de facto index in various spatial data processing systems, including PostGIS [4], Oracle Spatial [36], Apache Sedona [1], and SpatialSpark [72]. Given that these systems already maintain R-tree-based indexes, SwiftSpatial can directly leverage them for spatial joins, thereby avoiding additional index construction costs. Second, based on evaluation studies comparing various algorithms [64], the R-tree synchronous traversal stands out as one of the most efficient algorithms for spatial joins. Finally, although parallelizing synchronous traversal on CPU is not as straightforward as some other algorithms such as PBSM [51, 68], SwiftSpatial’s on-chip scheduler ensures fine-grained coordination between join units, facilitating low-overhead parallelization within synchronous traversal.

We evaluate SwiftSpatial on real-world and synthetic datasets of various size scales and compare it against a variety of CPU and GPU-based spatial data processing systems, including PostGIS [4], Apache Sedona [1], SpatialSpark [72], cuSpatial [3], and our multi-threaded C++ implementations of R-tree synchronous traversal and PBSM. Figure 1 showcases the speedups achieved by SwiftSpatial on 10-million-object datasets (OSM and Uniform) of different geometries (points and polygons). Overall, SwiftSpatial demonstrates outstanding performance and energy efficiency, achieving up to 5.36× latency reduction compared to the best-performing baseline system while consuming only 23.48W of power, 6.16× less than the baseline CPU. Moreover, the modular design of SwiftSpatial suggests it can not only be instantiated on data-center-grade FPGAs but also has the potential for deployment on embedded systems, showing its versatility and wide-ranging applicability.

The contributions of the paper are as follows:

- We design SwiftSpatial, a spatial join accelerator including:
 - Spatial join units with innovative hybrid parallelism.
 - Multiple efficient memory management units.
 - An on-chip spatial join scheduler that coordinates join units and memory management units.
- We implement SwiftSpatial on FPGA and adopt the R-tree synchronous traversal algorithm as the control flow.

- We compare SwiftSpatial with CPU and GPU-based spatial data processing systems on various datasets, showcasing its speedup of up to 5.36× compared to the best-performing baseline.
- We evaluate SwiftSpatial’s resource and power consumption, showing its deployment potential not only in data centers but also in edge spatial data management systems.

2 BACKGROUND AND MOTIVATION

2.1 Spatial Join

Let two datasets $R \subset \mathbb{R}^d$ and $S \subset \mathbb{R}^d$ consist of spatial objects in a d -dimensional space. A spatial join between R and S returns a set of all object pairs that meet a specific join predicate, such as *intersects* or *contains*. Equation 1 defines spatial join based on the *intersects* predicate. In practice, spatial joins are typically carried out in two or three-dimensional spaces, in which each object can have an arbitrary geometry, such as a point, circle, rectangle, etc.

$$R \bowtie_{\cap} S = \{(r, s) | r \in R, s \in S, r \cap s \neq \emptyset\} \quad (1)$$

A spatial join involves two steps: *filtering* and *refinement*.

Filtering. The filtering step aims to quickly identify potential candidate pairs of geometries that may satisfy the spatial predicate. To achieve this, the filtering step typically relies on either indexes like R-trees [27] and quadtrees [56] or data partitioning to prune non-relevant geometries efficiently and (b) approximate geometries with simpler structures such as *minimum bounding rectangles (MBRs)*. The filtering step returns the set of all object pairs from the two input sets whose MBRs intersect. This step may yield some false positives that satisfy the join predicate on approximated geometries but actually do not upon closer examination.

Refinement. The refinement step takes the results from the filtering step and verifies the actual spatial relationship between the candidate pairs [7, 25, 80]. To eliminate the false positives from the filtering step, this phase determines whether the pairs satisfy the given join predicate (e.g., intersects, contains, etc.) using the actual geometries instead of the MBRs.

The performance bottleneck in a spatial join depends on various factors such as data distributions, dataset sizes, and geometry complexities. For example, if most objects in the datasets are rectangles (equivalent to their MBRs) and the datasets are large, filtering out irrelevant pairs can be much more time-consuming than refinement [21, 36]. Conversely, if the object geometries are complex (e.g., intricate 3D objects), the refinement step may dominate the time spent on the spatial join pipeline [16, 69].

2.2 Indexes and Algorithms for Spatial Join

Extensive research has been conducted on spatial join algorithms. One category of approaches indexes or partitions one dataset and iterates over all objects of the other dataset as queries. Some representative indexes in this category include the R-tree [27], linearized KD-Trie [49], and simple grid [61]. Another category of approaches simultaneously evaluates both datasets. These approaches include plane-sweep [14], partition-based spatial-merge join (PBSM) [51], and R-tree synchronous traversal [8]. In this section, we delve into R-tree synchronous traversal and PBSM due to their great performance as shown in prior works [64, 68].

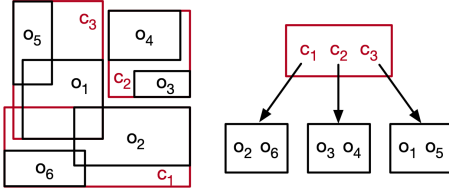


Figure 2: A two-level R-tree index containing six objects.

Algorithm 1: Synchronous Traversal

input : $RTree_R, RTree_S$
output: Spatial join result $\{(r, s) | r \in R, s \in S, r \cap s \neq \emptyset\}$
 ResultSet = RecursiveTraverse($RTree_R.root, RTree_S.root$)
return ResultSet

2.2.1 R-tree and Synchronous Traversal.

As visualized in Figure 2, an R-tree is a balanced tree structure. The tree has two types of nodes: directory nodes and leaf nodes. A directory node stores the MBRs and pointers to its child nodes, while a leaf node contains the MBRs and IDs of the spatial objects within the database.

An R-tree satisfies the following properties, considering that m and M represent the minimum and the maximum entries per node, respectively ($2 \leq m \leq \lceil M/2 \rceil$). First, all nodes, excluding the root, contain between m and M entries. Second, the root node may hold only one entry if the root is a leaf node and there is only one object in the dataset, while the upper bound M still applies. Third, all the leaf nodes have the same distance to the root node.

An R-tree can be constructed dynamically or statically. The original R-tree paper [27] manages tree construction by progressively inserting new objects into the tree. The R*-tree [6] enhances tree quality through more intricate insertion strategies. The advantage of dynamic insertion is its ability to intermix with queries and deletions. An alternative approach is to bulk-load the entire dataset to construct the R-tree, and the most widely-used approaches are Sort-Tile-Recursive (STR) [38] and Hilbert R-tree [33]. Bulk-loading produces superior R-tree topologies compared to dynamically constructed R-trees, improving query performance.

R-tree facilitates efficient spatial query processing by exploiting the hierarchical structure and MBRs to prune the search space. For instance, a window query on R-trees using an intersection predicate seeks to return all objects that intersect with the query geometry. R-tree handles such a query by starting the search from the root node and traversing the tree down to the leaf nodes. Given a directory node on the search path, all the MBRs of its children are evaluated to determine whether they intersect the query window. Only when an intersection is found will the traversal continue to explore the corresponding subtree. The objects on the searched leaf nodes are compared with the query window, and the qualified ones are returned as results.

Although a spatial join can be implemented by querying a dataset indexed by an R-tree with many window queries representing the objects from the other dataset, synchronous traversal using R-trees constructed on both datasets can yield better performance [8, 64].

Algorithm 2: Recursive Traversal

input : $Node_R, Node_S, ResultSet$
if $Node_R.isLeaf$ **and** $Node_S.isLeaf$ **then**
 | **for** $Obj_R \in Node_R, Obj_S \in Node_S$ **do**
 | | **if** $Obj_R.MBR \cap Obj_S.MBR$ **then**
 | | | ResultSet.add((Obj_R, Obj_S))
 | | **end**
 | **end**
end
else if $Node_R.isDirectory$ **and** $Node_S.isDirectory$ **then**
 | **for** $Child_R \in Node_R, Child_S \in Node_S$ **do**
 | | **if** $Child_R.MBR \cap Child_S.MBR$ **then**
 | | | TraverseRecursive($(Child_R, Child_S)$)
 | | **end**
 | **end**
end
else
 | **for** $Child_{Dir} \in Node_{Dir}$ **do**
 | | **if** $Node_{Leaf}.MBR \cap Child_{Dir}.MBR$ **then**
 | | | TraverseRecursive($(Node_{Leaf}, Child_{Dir})$)
 | | **end**
 | **end**
end
return

Synchronous traversal is an efficient spatial join algorithm [8]. It refers to the simultaneous traversal of two R-trees, one for each dataset being joined. The goal is to identify object pairs that potentially satisfy the join predicate by exploiting (a) the hierarchical structure of both R-trees and (b) MBRs associated with each R-tree node, such that the search space is pruned effectively.

Algorithms 1 and 2 summarize synchronous traversal on two polygon datasets using the intersect predicate. Starting at the root nodes of both R-trees, as shown in Algorithm 1, it proceeds in a depth-first search manner. Algorithm 2 details the procedure at each traversal step. If both inputs are leaf nodes, the object pairs satisfying the join predicate are added to the result set. If both inputs are directory nodes, the algorithm continues to explore the children pairs that satisfy the join predicate through recursive traversal of the qualified child nodes. If only one of the nodes is a leaf, the recursive traversal proceeds between the leaf node and the qualified children of the directory nodes.

2.2.2 Partition-Based Spatial-Merge (PBSM).

Contrary to synchronous traversal, PBSM joins spatial datasets without any index [51]. In the PBSM approach, both datasets are partitioned using a grid, wherein each tile in the grid collects all intersecting objects (each object may reside in multiple tiles). Thereafter, each tile undergoes a join sub-task, yielding results confined to that tile. These sub-tasks can be executed using either a nested loop join or a plane-sweep method. The results of all sub-tasks are merged as the final join results. PBSM can be straightforwardly mapped to multi-core CPUs [68] because (a) each sub-task can be executed independently and (b) duplicated results across partitions can be avoided by reporting a result pair only in one tile [15].

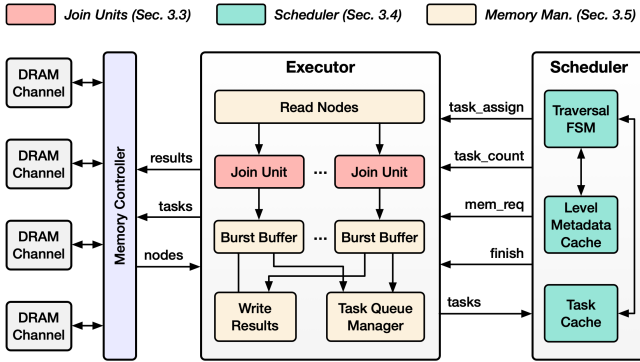


Figure 3: SwiftSpatial accelerator overview.

2.3 Optimizing Spatial Join Performance

Over the past four decades, researchers have extensively studied spatial join algorithms, thus, further improvements by algorithm innovations have become increasingly challenging. Therefore, to enhance spatial join performance, system implementations have become increasingly important [60]. This can be achieved by either increasing system resources allocated to the join or boosting efficiency per compute unit through hardware acceleration.

Approach 1: scale-up and scale-out. Scaling up spatial join on a single server involves harnessing the power of multi-core CPUs [48]. For further system performance improvements, one can use big data frameworks for spatial data to scale out spatial join operations [19, 50], such as SpatialSpark [73], LocationSpark [66], SpatialHadoop [18], HadoopGIS [5], and Simba [70]. However, neither the scale-up nor the scale-out solution improves the spatial join efficiency, as the increased performance comes at the expense of additional computing resources.

Approach 2: hardware acceleration. Researchers have been exploring the use of hardware accelerators such as GPUs to speed up spatial joins. GPUs are well-suited for some types of spatial queries, as their graphics primitives operating on polygons align closely with spatial objects [16, 17]. Specifically, the GPU can map polygons into pixels through rasterization [65, 75] and perform spatial operations, such as intersection checks, at the pixel level. This approach is particularly effective for the refinement step in the spatial join pipeline, as GPUs have significant advantages over CPUs when dealing with highly complex polygons.

However, GPUs have not been shown to be suitable for the filtering step of spatial joins. For synchronous traversal, the complex control flow does not align well with the many-core GPU architecture. Even for simpler cases of batched window queries on R-trees [43, 53, 71], GPUs face significant challenges regardless of whether adopting BFS or DFS. In DFS, each GPU thread is responsible for a single query window, leading to significant workload imbalances between threads, thus the performance is limited by the slowest thread. In BFS, memory management becomes challenging since the number of result pairs produced by a thread block is unknown beforehand. Neither memory overflow nor reserving a huge amount of memory per thread block is ideal. The former leads to execution failures while the latter limits the number of concurrently running thread blocks. If one would map PBSM to

GPUs, the join workload across different tiles can be highly skewed: the imbalance loads between streaming multi-processors can collapse the GPU’s performance [63]. Besides, the problem of using an additional computation pass for appropriate memory allocation in R-trees remains in PBSM.

2.4 Motivation and Goal

We aim to improve the performance and efficiency of in-memory spatial join, particularly the filtering step, by rethinking computer architecture designs, given that it is challenging to solve the problem via algorithm innovations or utilizing existing accelerators, as discussed in the previous section.

3 SWIFTSPIATIAL

In this section, we first outline the design principles for an efficient spatial join accelerator (§3.1) and overview SwiftSpatial (§3.2). Subsequently, we delve into the key components of SwiftSpatial, including the join units (§3.3), the on-chip scheduler (§3.4), and the memory management units (§3.5). Next, we describe SwiftSpatial’s FPGA implementation (§3.6). Finally, we discuss the approaches to incorporate SwiftSpatial into spatial data management systems (§3.7).

3.1 Design Principles

As introduced in §2, spatial join algorithms commonly decompose the join process into many sub-join tasks on tiles of objects (e.g., nodes in R-trees or tiles in PBSM). Consequently, an efficient accelerator for spatial joins should meet three fundamental criteria:

- Swift execution of each sub-join on a tile pair.
- Parallelization of sub-join tasks by using multiple join units.
- Minimal task parallelization overhead even when dealing with complex control flows like R-tree synchronous traversal.

3.2 Accelerator Overview

Reflecting the aforementioned criteria, we design *SwiftSpatial*, an in-memory spatial join accelerator for the filtering phase.

SwiftSpatial instantiates multiple specialized join units for the efficient joining of object tiles. The join units implement nested loop join rather than plane sweep for the following reasons. While plane sweep — designed to minimize the number of predicate evaluations through sorting — is a frequent choice in software solutions, this preference stems from the slow predicate evaluations on CPUs. In contrast, with our proposed architecture employing hybrid parallelism, predicate evaluations between objects become notably faster, even if each evaluation involves multiple object boundary comparisons. Furthermore, the efficiency of plane sweep depends on data distributions and tile sizes. Specifically, its performance often lags behind the nested loop join on datasets with overlapped objects or when utilizing small tiles, as we will illustrate in §4. Finally, plane sweep is a sequential algorithm that benefits more from a high clock frequency than from a parallel hardware architecture.

Another key accelerator component is the on-chip scheduler that manages the join control flow and the coordination of the join units. Executing the control flow on-chip results in low performance overhead compared to the alternatives like relying on an external CPU for control signal transmission. In this paper, we incorporate

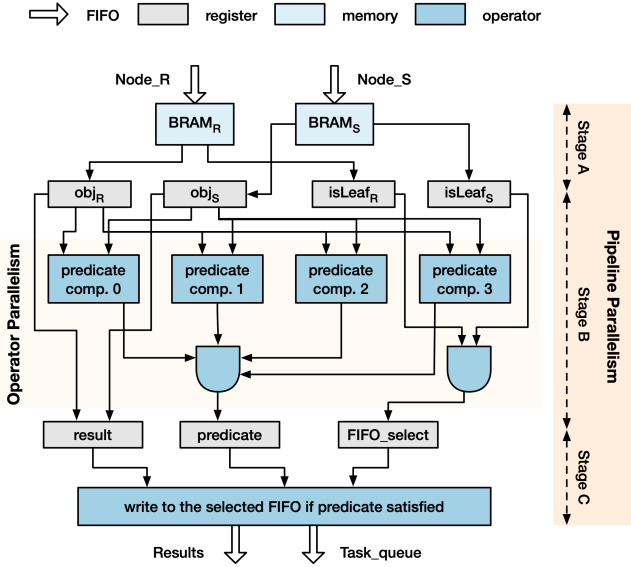


Figure 4: The microarchitecture design of a join unit.

R-tree synchronous traversal into the scheduler, showcasing the execution of a complex control flow in SwiftSpatial. The integration of R-tree synchronous traversal also allows SwiftSpatial to leverage the existing R-tree indexes maintained by spatial data management systems, such as PostGIS [4], Oracle Spatial [36], Apache Sedona [1], and SpatialSpark [72], avoiding additional index construction costs during spatial joins.

Figure 3 overviews SwiftSpatial. Beyond the join units and the on-chip scheduler, SwiftSpatial encompasses a set of memory management units, which optimize data transfer between the accelerator and DRAM. On-chip communication between function units, like the join units and the scheduler, is facilitated by FIFOs, akin to pipes in a software context.

3.3 Join Units

A join unit processes a pair of nodes from the two R-trees being joined and generates all intersected entry pairs.

Figure 4 shows the microarchitecture design of a join unit. The input node pairs are streamed into the join unit through two FIFOs. A join unit consists of two on-chip SRAM slices used to store the pair of input nodes. During each iteration of the join process, a pair of objects from the nodes are read from SRAM into registers. Then, multiple comparators are employed to assess whether the MBRs intersect, where all the comparators work in parallel. Specifically, there are four comparisons for 2-dimensional MBRs: $r.right \geq s.left$, $s.right \geq r.left$, $r.top \geq s.bottom$, $s.top \geq r.bottom$, where r and s are two entries from the pair of input nodes. If all the comparison outcomes are true (evaluated by the AND gate), the pair of objects will be written to one of the output FIFOs. If both nodes are leaf nodes, the pair is written to the final result FIFO; otherwise, it is written to the task queue FIFO.

A join unit processes a pair of objects per cycle, thanks to the hybrid parallelism in the architecture. As shown in Figure 4, the first level of parallelism is operator parallelism. The

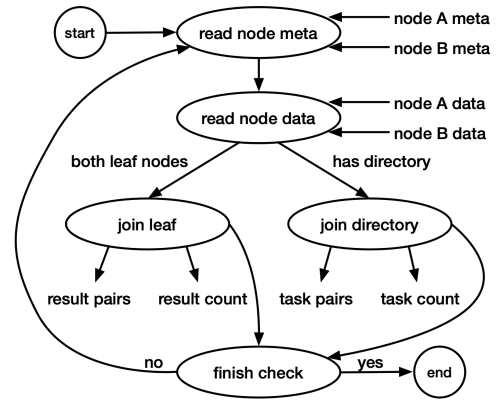


Figure 5: The control flow of a SwiftSpatial join unit.

combinational logic that evaluates different comparisons simultaneously and aggregates the comparison results can be completed within a clock cycle. Another form of parallelism is pipeline parallelism. Figure 4 shows different levels of registers in the pipeline. In the first stage of the pipeline, the objects are read from SRAM into the object registers. In the second stage, whether the MBRs intersect is evaluated. In the final stage, the qualified results are written into FIFOs. Thus, there are three object pairs in progress within the pipeline, allowing one pair of objects to be introduced into the pipeline every single clock cycle.

Figure 5 demonstrates the control flow of a hardware spatial join unit. The join unit follows a series of steps until it receives the finish signal. Initially, it receives node metadata from the read unit, which indicates the number of node entries and whether it is a leaf or directory node. Based on this information, the join unit reads the corresponding node data. Once the reading process is complete, the join procedure starts. During the procedure, the join unit examines every pair of entries between the node pair and checks if they intersect, outputting the qualifying pairs. If both input nodes are leaves, the outputs are recorded as results; otherwise, the generated node pairs are treated as tasks for future join operations. After joining the entries, the join unit checks if there is a finish signal sent from the scheduler, and it proceeds with the next pair of nodes if it has not received one.

3.4 On-chip Scheduler

Although one potential approach to managing synchronous traversals is to combine the hardware node-level joins with a software control flow, this method is too time-consuming, because it necessitates many accelerator kernel invocations and frequent data transfers between the host server and the accelerator.

To overcome this, SwiftSpatial incorporates a dedicated hardware scheduler, which manages the synchronous traversal procedure and coordinates all function units, including the read and write units, join units, and the task queue manager.

We modify the synchronous traversal algorithm to adopt BFS, maximizing task-level parallelism among the join units. This is essential because the original synchronous traversal, as illustrated in Algorithm 2, employs a depth-first search (DFS), which allows joining only one node pair at a time and fails to fully leverage the parallelism capabilities of SwiftSpatial. By contrast, the BFS

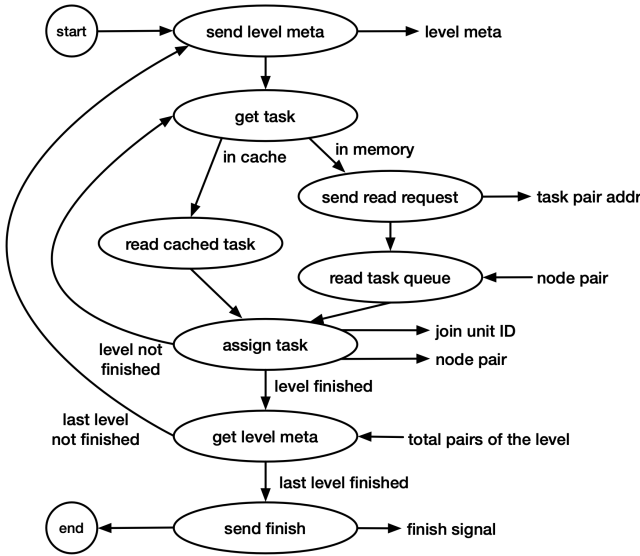


Figure 6: The control flow of the on-chip scheduler.

synchronous traversal [31] performs the join level by level, such that the tasks in each level can be easily parallelized. At each level, the scheduler considers all pairs of nodes to join and assigns the tasks to the join units. For instance, at the root level, the sole pair of nodes to join is the pair of roots. The scheduler assigns the join task to the first join unit and waits for the result to be written to memory by the task queue manager. Assuming the roots are not leaf nodes, all the results generated by joining the roots become tasks for the second level, and the scheduler assigns these tasks to the join units. This process continues until all tasks at the leaf level are completed, and the results are written back to memory.

Figure 6 details the workflow of the scheduler. To start the BFS synchronous traversal in a level, the scheduler sends the physical addresses to the task queue manager to inform it where to begin writing the intermediate results (future tasks). Next, it starts dispatching jobs to the join units. To accomplish this, it requests the results from the previous level from the task queue manager. Because the task queue manager needs to read the requested task (a pair of nodes) from memory, which involves a random DRAM access, we optimize memory bandwidth utilization by implementing burst loading: reading a sequence of node pairs that can be issued next and caching them in the scheduler’s SRAM. As a result, the scheduler only needs to send a request to the task queue manager when its local cache is empty. After obtaining the node pair as a task, the scheduler looks for a join unit to assign the task. Specifically, the scheduler dispatches tasks to the join units in a round-robin manner. With the node pair and join unit ID, the scheduler sends this information to the read unit, which loads the node pair from memory and passes the data to the respective join unit. The task assignment continues until all the tasks on the current level are completed. The task queue manager then sends the scheduler the number of pairs produced in the current level, allowing the scheduler to determine the starting physical address to write from in the next level. The aforementioned procedures are repeated until the leaf level is completed. The scheduler finally sends a finish signal to other function units, indicating all tasks have been dispatched.

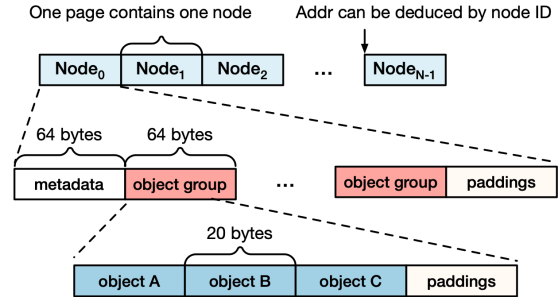


Figure 7: Data format of a serialized R-tree in SwiftSpatial.

3.5 Memory Management

SwiftSpatial directly manages the physical address space. While it increases design complexity, SwiftSpatial avoids the overhead associated with dynamic memory allocation, deallocation, and page table management existing in virtual memory management. Meanwhile, the memory management unit can burst the read and write requests, thus optimizing the memory bandwidth utilization.

Serialized R-tree data format. Figure 7 illustrates the serialized R-tree data format used in SwiftSpatial. As introduced in §2, an R-tree node can contain up to M entries. We allocate exactly one page to store a node and set the page size large enough to accommodate M entries and the node’s metadata. Since the AXI interface between the accelerator and the memory controller has a maximum data width of 64 bytes, SwiftSpatial aligns the pages to be multiple of 64 bytes and stores data in 64-byte units. Within a page representing an R-tree node, the first 64-byte block contains the node’s metadata, while the data blocks store the objects or children within the node. The metadata includes the node ID, the entry count, the node type (leaf or directory), and the node’s MBR. A data block can hold three objects or children, each consisting of a 4-byte integer ID and four 4-byte floating point numbers representing the MBR boundary (left, right, top, and bottom). The pages are sorted in ascending order based on the node IDs. With a fixed page size, SwiftSpatial can infer the physical address of a node using the node ID.

Optimizing bandwidth utilization via request bursting. While reading nodes exhibit a sequential memory access pattern (multiple consecutive 64-byte blocks), the write requests in the accelerator can be highly random. This randomness arises from join operations, where, for example, it may take a join unit several cycles to output the second pair of intersected objects after the first is sent. Several join units can interleave write requests, with each write being only 8-byte long (a pair of integer object IDs).

To solve this problem, we introduce a burst buffer after every join unit. The burst buffer takes the join results as input and sends a burst of results to the task queue manager or the result write unit. The burst buffer will output a burst either when the accumulated results reach a size threshold, e.g., 4 KB, or when it is the end of joining a pair of nodes. The write result unit or the task queue manager pulls the burst results from the burst buffers in a round-robin fashion and writes the data to DRAM sequentially.

Task queue manager. According to the scheduler’s requests, the task queue manager writes the intermediate results (node pairs on non-leaf levels that intersect) as future tasks to memory or reads node pairs to be joined from memory.

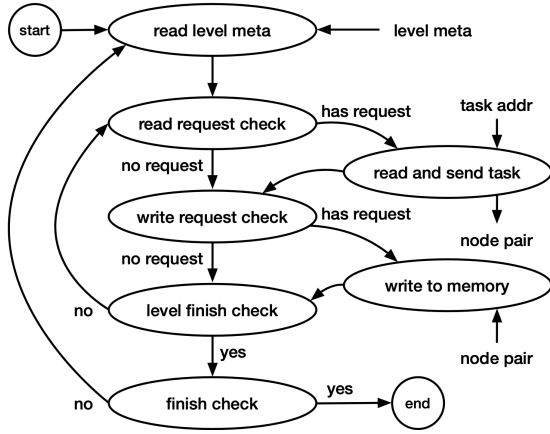


Figure 8: The control flow of the task queue manager.

The task queue manager workflow is illustrated in Figure 8. It starts by receiving the level metadata from the scheduler, which indicates the number of join tasks in the current level and the starting physical address for storing intermediate results. Next, it checks for any read requests from the scheduler and returns the corresponding node pairs. Subsequently, the task queue manager pulls data from the burst buffer and writes these intermediate results to memory in bursts. The process continues until the manager receives a level finish signal at the leaf level.

3.6 FPGA Implementation

We select prototype SwiftSpatial on FPGAs for two primary reasons: (a) it facilitates direct performance evaluation of the accelerator in contrast to the simulation-based approach, and (b) the widespread adoption of FPGAs in data centers makes SwiftSpatial readily integrable with spatial data management systems [2, 22, 39, 45, 77].

We developed SwiftSpatial in Vitis HLS 2022.1 using C/C++ and set the accelerator’s clock frequency as 200 MHz. The on-chip memory (SRAM) and FIFOs in SwiftSpatial correspond to BRAMs on the FPGA, supporting a read or write request every clock cycle, while registers are mapped to Flip-Flops (FFs). The FPGA’s digital signal processors (DSPs) execute floating-point operations, with other logic operations facilitated via lookup tables (LUTs).

3.7 System Integration

A spatial data management system leveraging SwiftSpatial would adopt a hybrid CPU-accelerator architecture. The CPU constructs and maintains spatial indexes (e.g., R-trees) or partitions (e.g., PBSM) and handles non-join queries such as window queries, while the accelerator processes spatial join queries. Upon receiving a spatial join query, the up-to-date indexes are transferred to the accelerator, which then processes and returns the join results.

There are two ways to integrate CPUs and accelerators as an accelerated spatial data management system:

Operator offloading. In this approach, the CPU server operates a data management system while the accelerator serves as an offloading engine. An example of this offloading architecture is Alibaba’s cloud-native database engine PolarDB, which accelerates LSM-trees (log-structured merge trees) by offloading compactions to FPGAs [30, 77].

Accelerator-as-a-Service. SwiftSpatial can function as a cloud-based service accessible to multiple users, avoiding the cost of integrating an accelerator per DBMS. Users can submit spatial join queries to the service, either by providing raw datasets or serialized R-trees. The host server of SwiftSpatial processes the user’s requests from the network, constructs indexes if needed, forwards the queries to the accelerator, and returns the results to the users. An example of accelerator-as-a-service in the cloud is SAP DASH [45], which presents the FPGA as a hardware data processing service to a cluster of databases, delegating the asynchronous execution of compute-intensive database operations.

In this paper, we evaluate SwiftSpatial using the offloading model, and the system can be easily extended to the accelerator-as-a-service model by adding a network interface on the host server.

4 EVALUATION

We evaluate SwiftSpatial on real-world and synthesized datasets and compare it to a wide range of CPUs and GPUs-based spatial join implementations. We show that SwiftSpatial outperforms the most performant software baseline by up to 5.36× in terms of latency, while requiring 6.16× less power. The modular architecture of SwiftSpatial facilitates its deployment not only on data-center-grade FPGAs but also on embedded systems, showcasing its adaptability and potential for broad applicability.

4.1 Experimental Setup

4.1.1 Datasets.

We evaluate SwiftSpatial on both real-world and synthesized datasets. For real-world datasets, we use the Open Street Maps (OSM) dataset made available by SpatialHadoop [20]. Specifically, we process its *buildings* subset for polygon generations (converted to MBRs) and use the *all nodes* subset for point objects. The dataset scales range from one hundred thousand to ten million objects, and we produce two different datasets for the spatial join operation. We also produce synthesized datasets of rectangles in uniform distribution. Specifically, we set the map size as 10K by 10K, within which each unit-square object is randomly and uniformly distributed.

4.1.2 Software.

For CPU baselines, we evaluate open-source software and our C++ multi-threaded synchronous traversal and PBSM implementations.

The open-source software baselines include PostGIS [4], Apache Sedona [1], and SpatialSpark [72], thus covering both spatial database and spatial big data frameworks. PostGIS is a spatial database that extends PostgreSQL with spatial functionalities. Apache Sedona, previously known as GeoSpark [74], is a system for processing large-scale spatial data. Even on a single server, Sedona carries out spatial joins on multiple-core CPUs by partitioning the data, performing join on each partition, and subsequently merging the results. Similar to Sedona, SpatialSpark is an academic big spatial data framework developed on top of Apache Spark [76]. All the CPU baseline software above performs spatial join using R-trees.

We implement multi-threaded C++ spatial join baselines, including R-tree synchronous traversal and PBSM. Our implementations are adapted from the single-threaded artifacts in [64]. For synchronous traversal, we implement two multi-threaded versions using OpenMP. The first version applies a BFS traversal, identical to the

FPGA implementation illustrated in §3.4. At each level of the BFS traversal, we consider the node pairs for joining as tasks to be assigned to various threads. Each thread is responsible for a subset of tasks, with a single thread subsequently merging the results. The second version combines DFS with BFS. The idea is to start the search with multi-threading BFS, and, once the number of node pairs to join surpasses the number of threads significantly, these tasks are dispatched to different threads. These threads manage the tasks using the conventional DFS synchronous traversal, after which a single thread merges the results. Specifically, when the task count is at least ten times greater than the hardware thread number, the algorithm switches to DFS. This is because assigning only one task per thread can lead to significant workload imbalances due to the varying DFS traversal time per task. For both BFS and BFS-DFS implementations, we evaluate two OpenMP scheduling strategies, static and dynamic, and report the best performance. The static schedule assigns the same number of tasks to each thread, while the dynamic schedule does not assume the number of tasks per thread and assigns a task to a thread as soon as it is idle. Our multi-threaded PBSM based on OpenMP supports arbitrary partition numbers and uses plane sweep to join the tiles. We adopt the one-dimensional PBSM, which partitions the data in one dimension and sweeps the data in the other dimension, because it has shown superior performance compared to the two-dimensional PBSM [68].

For GPU evaluations, we use cuSpatial [3], the only open-source GPU-based spatial join library we found. However, cuSpatial only supports Point-in-Polygon tests (points join polygons using the within predicate) rather than joining two polygon datasets. Consequently, we restrict our GPU evaluations to these queries. Besides, cuSpatial employs quadtrees rather than R-trees as the index, because the boundaries of quadtree nodes can be computed simply with knowledge of the tree’s levels and the node ID. However, this comes at the expense of an inferior indexing quality compared to R-trees [36]. The quadtree index is only constructed on the point dataset, and the Point-in-Polygon queries are performed through the use of polygon batches serving as window queries.

4.1.3 Hardware.

The baseline CPU server contains an AMD EPYC 7313 16-core processor (7 nm) with a base frequency of 3 GHz and 256 GB of DDR4 memory. We run cuSpatial on an A100 SXM4 GPU (7nm) with 40 GB high-bandwidth memory (HBM). We evaluated SwiftSpatial on an AMD Alveo U250 FPGA (16 nm) equipped with 64 GB of DDR4 memory (4 x 16 GB). Since both a CPU core and an FPGA join unit are responsible for joining a pair of nodes during R-tree synchronous traversal, we instantiate 16 join units on the FPGA to compare against the 16-core CPU.

4.2 End-to-end Spatial Join Performance

We compare the end-to-end join latency between SwiftSpatial and the baseline CPU and GPU systems. This assessment assumes pre-constructed indexes on both datasets, with associated costs reported separately in §4.8. For FPGA experiments, the join latency includes the join operation (kernel) and data movement (index and results) between the CPU and FPGA. For baselines, we measure only the join latency itself: the data and indexes are already loaded in memory

(or GPU memory), and, for big data frameworks and PBSM, the data is already partitioned.

We report the best baseline and FPGA performance using the following configurations. For C++ multi-threaded synchronous traversal, we tune parameters, including node sizes, traversal strategies, and OpenMP scheduling policies. After evaluating different traversal and scheduling strategies, we find that a combination of BFS and dynamic scheduling provides the best performance in the majority of our experiments. For both SwiftSpatial and the C++ synchronous traversal, the maximum R-tree node size (the number of entries a node can accommodate) is set to 16, which is shown to be optimal in a later section (§4.3). For C++ multi-threaded PBSM, we evaluate different partition numbers ($10^2 \sim 10^5$) and partition-sweep directions (partition in one direction and sweep in the other) and report the best performance. With PostGIS, we configure the maximum parallel worker processes to 16, aligning with the available number of CPU cores on the server. For SpatialSpark, we assess varying numbers of partitions and find that the optimal setting is 64. In the case of cuSpatial, we fine-tune the average leaf node size in the quad-tree and set it as 128 for our experiments eventually. Since cuSpatial processes spatial join as window queries on the indexed point datasets, we use a batch size of 20K, such that the throughput is maximized without overflowing the GPU memory.

SwiftSpatial achieves significant speedup over all baselines. Specifically, it outperforms the multi-threaded synchronous traversal by 1.41~5.36 \times , the multi-threaded PBSM by 2.60~28.69 \times , the single-threaded C++ implementation by 16.21~51.57 \times , the single-threaded PBSM by 27.66~125.96 \times , PostGIS by 47.07~493.36 \times , Apache Sedona by 21.07~360.70 \times , SpatialSpark by 46.94~1411.21 \times , and cuSpatial by 168.93~1291.49 \times .

As shown in Figure 9, the multi-threaded synchronous traversal consistently performs best among the baseline systems, except for Uniform 10Mx10M polygons for which PBSM has a slight edge. While PBSM showcases near-linear scalability on Uniform datasets (15.8x latency reduction with 16 cores for 10Mx10M polygons), the single-threaded performance of PBSM lags behind that of synchronous traversal (same observation as in [64]), thus PBSM, in the best case, can only match the performance of synchronous traversal with 16 cores. However, PBSM’s scalability depends on data distributions: the scalability falters on OSM datasets with a skewed object distribution, even with large partition numbers. Despite leveraging multi-core capabilities, PostGIS and the two big data frameworks tend to underperform single-threaded C++ synchronous traversal. This underperformance might be attributed to the overhead of abstractions and, for the big data frameworks, inefficiencies related to Scala compared to C++ and the data shuffling costs.

CuSpatial, despite being GPU-based, proves to be one of the slowest baselines, even underperforming the single-thread C++ implementations. For the GPU performance measurement, we already indexed the datasets and copied the data to the GPU memory prior to measuring the join performance. The low performance may stem from several factors. Firstly, the quadtree index implemented on the GPU is of lesser quality compared to R-trees [36]. Secondly, cuSpatial only supports indexing for one dataset since it only supports point indexing. Consequently, polygons are processed as batch queries, resulting in less efficiency compared to synchronous traversal with both datasets indexed. Third, without

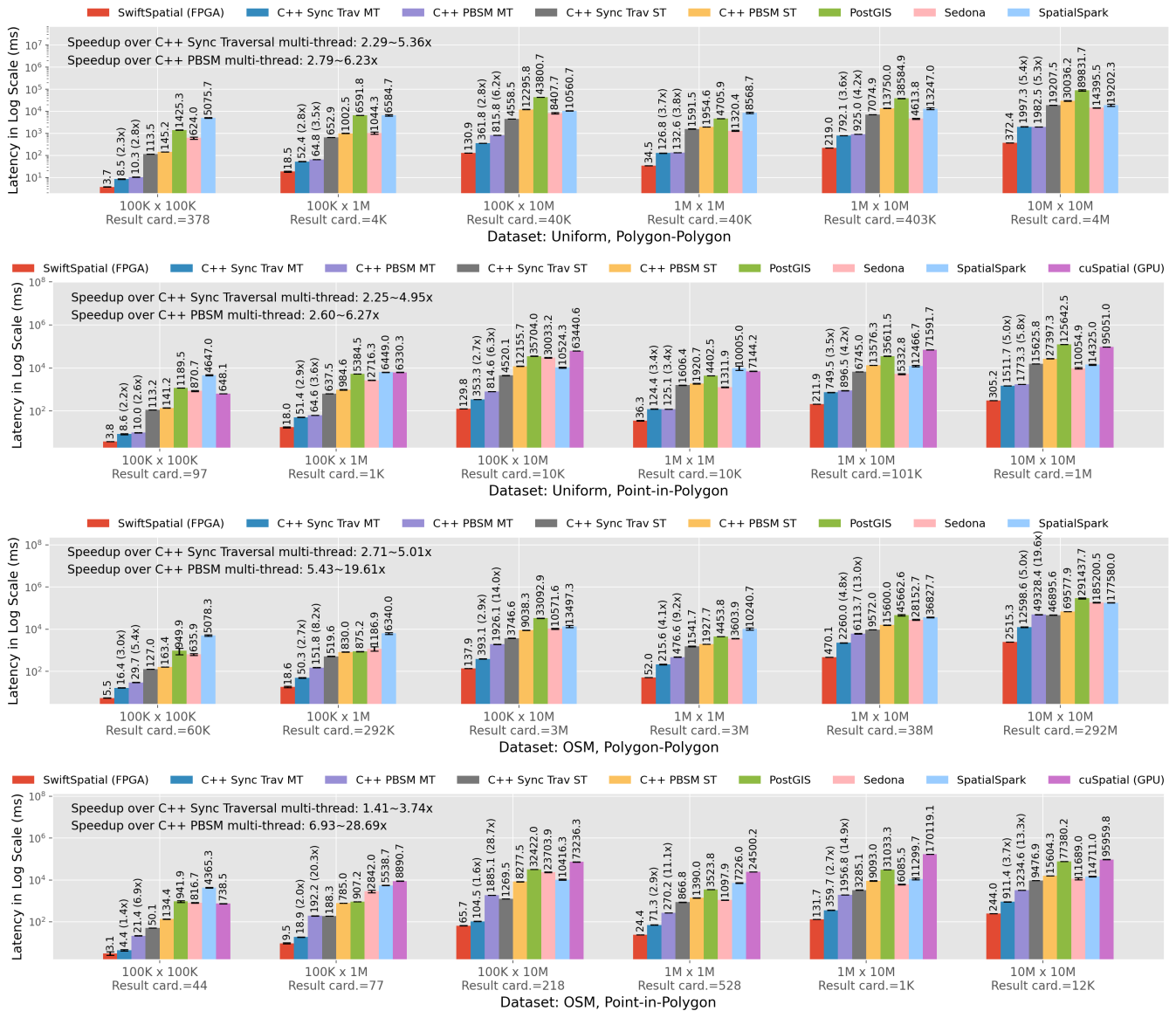


Figure 9: End-to-end spatial join performance on different datasets, data scales, and geometries.

knowing the number of join results in advance, cuSpatial resorts to over-allocating memory, limiting query batch sizes. For example, even though none of the datasets evaluated produce more than 300 million result object pairs (well below the 40 GB of GPU memory), the maximum batch size that passed all tests is only 20K. This limitation results in sub-optimal GPU core utilization.

4.3 Effect of R-tree Node Sizes

We investigate the impact of varying R-tree node sizes, defined as the maximum number of objects or children a node can contain, on spatial join performance on CPU and FPGA. Typically, smaller node sizes can result in more efficient search space pruning during synchronous traversal, thereby reducing the total number of predicate evaluations. However, this comes at the expense of increased

random memory accesses to read more small nodes. For example, for polygon joins on the OSM 1M dataset, node sizes of 8, 16, and 32 lead to the reading of 524K, 244K, and 119K node pairs (decreasing random memory accesses), while evaluating 33M, 62M, 122M predicates between MBRs (increasing computation), respectively.

Figure 10 shows the impact of node sizes on performance for both the 16-thread C++ synchronous traversal and the 16-join-unit accelerator. Both systems reach peak performance with a node size of 16. Despite smaller node sizes offering enhanced efficiency in pruning the search space, the increase in random memory accesses restricts the rate at which node pairs can be loaded into the processor or the accelerator. Conversely, with larger node sizes, the effectiveness of space pruning decreases, leading to more predicate evaluations between node pairs throughout the traversal.

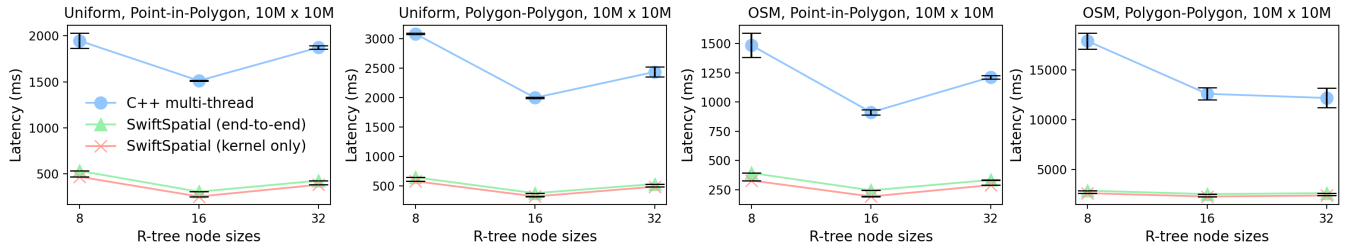


Figure 10: The effect of different R-tree node sizes on spatial join performance given 16 threads or 16 join units.

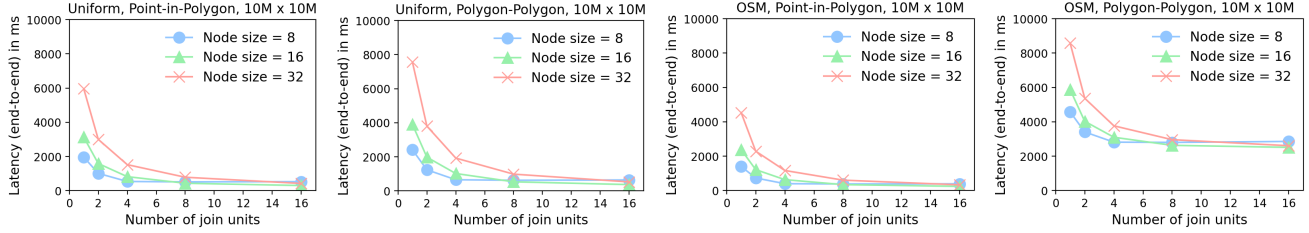


Figure 11: The effect of R-tree node sizes when instantiating different numbers of join units.

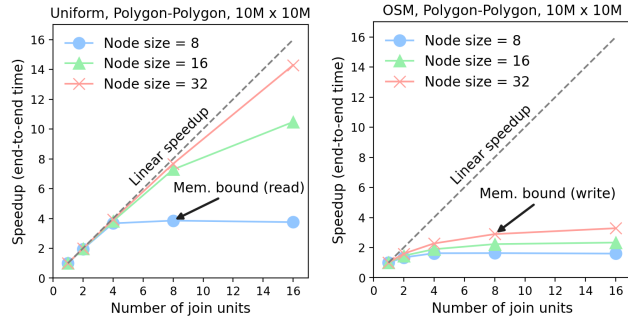


Figure 12: The performance scalability of the join units using different node sizes.

4.4 Performance Scalability of the Join Units

We evaluate the performance scalability of the join units by instantiating one to sixteen units on SwiftSpatial. We first examine the impact of varying node sizes in relation to different numbers of join units. Subsequently, we evaluate the performance scalability across a range of node sizes.

The selection of optimal node sizes is related to the number of instantiated join units. Figure 11 compares the end-to-end join performance using different datasets and node sizes. For instance, in the Point-in-Polygon join on the Uniform dataset, the accelerator with a single join unit optimally favors a smaller node size of eight. As the quantity of join units escalates to eight, a node size of 16 emerges as the optimal selection. With an accelerator comprising 16 join units, a node size of 16 still retains its optimal status; however, the performance disparity between node sizes of 16 and 32 diminishes significantly (305ms and 425ms, respectively). The rationale behind this lies in the fact that, when a lesser amount of join units are instantiated, the computation resources dedicated to predicate evaluation are restricted, thereby making R-trees with smaller nodes a more desirable choice due to their potential to reduce computation effectively. Contrarily, when there is a substantial number of join units instantiated, these units end up competing for memory access. Consequently, synchronous traversal with smaller

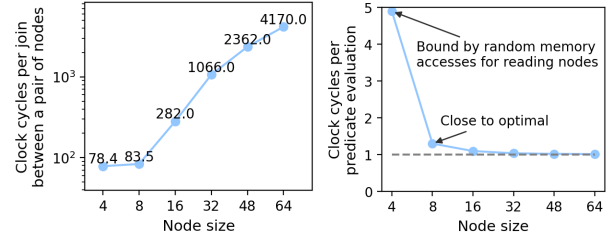


Figure 13: A join unit can achieve near-optimal performance.

nodes becomes memory-bound, leading to a situation where some units are idle, waiting for data.

As node size increases, the performance scales better with the number of join units. Figure 12 shows the speedup obtained by instantiating multiple join units. For the Uniform dataset, which yields fewer results, the performance plateaus after instantiating four units when using a node size of 8. Conversely, with a node size of 32, the performance continually increases by adding more units, demonstrating an almost linear progression up to 16 join units. With the OSM dataset, which yields a greater number of results, the join performance is inherently limited by the write performance determined by memory bandwidth, even though the computation can still be accelerated by instantiating more units.

4.5 How Good is a Hardware Join Unit?

In addition to the end-to-end performance evaluation, we microbenchmark the hardware join units in SwiftSpatial, specifically focusing on their efficiency in evaluating join predicates between nodes. For this purpose, we constructed an accelerator with a single join unit and fed R-tree node pairs of varying sizes into it.

The join unit nearly achieves the ideal performance rate of one predicate evaluation per cycle. Figure 13 shows the join unit performance given different node sizes. The plot on the left presents the number of clock cycles needed to perform a join between a pair of nodes, which includes the time needed for reading the data and evaluating the predicates. The plot on the right normalizes the performance as the average number of cycles needed

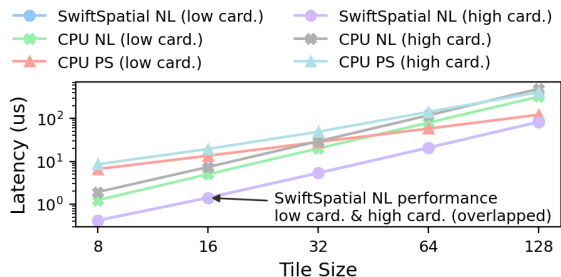


Figure 14: Comparison between nested loop (NL) and plane sweep (PS) with different tile sizes and result cardinality.

per predicate evaluation. For instance, if both nodes contain 32 entries, then 32^2 predicates are evaluated during the join operation. If this operation takes 1066 cycles to complete, then the number of cycles per predicate evaluation is $1066/32^2 = 1.04$. As shown in the plot on the right, the performance of joining small nodes (with four or fewer entries) is constrained by the random DRAM accesses to fetch the input node pairs. Conversely, the performance is close to the optimal value (one predicate evaluation per cycle) when a medium-sized node (eight or more entries) is employed. Here, the cycles per predicate range from 1.02~1.30 using node sizes of 8~64.

The SwiftSpatial join unit exhibits a significant advantage over software-based nested loop join or plane sweep. Figure 14 compares the latency of tile-level joins across varying tile sizes and result cardinalities, given a single SwiftSpatial join unit and a single-threaded C++ implementation. To modulate result cardinalities, we adjusted the edge lengths of the tiles and populated them with unit-length rectangles. As a reference, the low-cardinality configuration yields no results for tile sizes under 128, while the high-cardinality setup produces 2170 results when joining 128-object tiles. Several observations can be made from Figure 14. Firstly, even software nested loop join outperforms plane sweep for small and moderate tile sizes (less or equal to 32 and 64 for the low and high cardinality experiments, respectively). Secondly, the performance of plane sweep is more susceptible to data distributions, as the increasing number of objects in the sweep queues can substantially hinder its efficiency. Thirdly, the SwiftSpatial join unit performance is consistent regardless of result cardinalities, as shown by the overlapped performance curve in Figure 14. Lastly, the fast predicate evaluation facilitated by the hardware join units leads to a significant performance advantage over software nested loop and plane sweep up to a moderate tile size (128), which is around an order of magnitude greater than typical R-tree node sizes.

4.6 Hardware Resource Consumption

Table 1 shows the hardware resource usage of SwiftSpatial, configured with different numbers of join units in the kernel. The kernel stands for user-space logic, while the shell refers to the FPGA infrastructure, including the memory controller, the PCIe controller, etc., consuming a constant amount of resources. The resource consumption is classified into four categories: Lookup Tables (LUTs) used for combinational logic, Flip-Flops (FFs) functioning as registers, Block RAMs (BRAMs) serving as on-chip memory, and Digital Signal Processors (DSPs) responsible for floating-point operations.

Table 1: SwiftSpatial consumes few FPGA resources.

	LUT	FF	BRAM	DSP
Kernel (1 PE)	0.67%	0.44%	2.46%	0.16%
Kernel (2 PE)	0.87%	0.55%	3.65%	0.21%
Kernel (4 PE)	1.24%	0.75%	6.03%	0.34%
Kernel (8 PE)	1.96%	1.13%	10.79%	0.60%
Kernel (16 PE)	3.35%	1.60%	28.05%	1.12%
Shell	10.89%	9.21%	14.96%	0.11%
Shell + Kernel (16 PE)	14.24%	10.81%	43.01%	1.23%
FPGA Total	1,728,000	3,456,000	2,688	12,288

On a data center FPGA such as U250, an accelerator kernel equipped with 16 join units consumes less than 30% of the total hardware resources. Notably, the most substantial resource consumption is Block RAMs (BRAMs), accounting for 28.05% of the total resources, while other resources are far less utilized (below 4%). This is attributed to the fact that each join unit in SwiftSpatial requires minimal resources (LUT, FF, and DSP), while the FIFOs interconnecting the join units, burst buffers, and read and write units all demand BRAM slices. These FIFOs are used to buffer data within the processing pipeline, thereby minimizing stalls.

SwiftSpatial, when configured with a smaller number of join units, can be deployed on embedded FPGAs for edge spatial computing. For example, PYNQ Z2, one of the lowest-end CPU-FPGA SoC on the market, contains 106,400 FFs, 53,200 LUTs, 140 BRAMs, and 110 DSPs. Assuming that 60% of these resources can be allocated for user kernels, it would be feasible to host a SwiftSpatial kernel comprising one to two join units. By optimizing BRAM usage, such as employing shift registers in place of BRAMs to construct the FIFOs, it becomes possible to instantiate a SwiftSpatial kernel with up to four join units on the PYNQ Z2.

4.7 Power Consumption

We compare the power consumption between CPU, GPU, and FPGA for spatial join. For CPU, we measure the multi-threaded C++ implementation as it is the most performant software baseline; and we measure the GPU power consumption when running cuSpatial. In both cases, we executed the Point-Polygon join on the OSM 10M dataset continuously using a while loop and assessed the power using AMD RAPL (Running Average Power Limit) and NVIDIA System Management Interface, respectively. For the FPGA, we used Vivado to report the accelerator’s power consumption.

Despite its superior performance, the power consumption of SwiftSpatial is only 23.48W, 6.16× lower than the CPU and 4.04× lower than the GPU. Thanks to the modest hardware resource utilization of SwiftSpatial (§4.6), the accelerator manages to sustain high performance while using minimal energy. The CPU power consumption (144.69W) is close to its Thermal Design Power (TDP) of 155W, indicating that the cores are fully utilized during the join operation. Contrarily, the GPU, despite having a 400W TDP, consumes only 95.01W during the join. This discrepancy likely stems from significant under-utilization of the many GPU cores: the substantial memory usage of cuSpatial limits the batch sizes during the join operation, thus restraining the core usage.

Table 2: Time consumption of joins versus index constructions from scratch on ten-million-object datasets.

	Indexing	Join (C++)	Join (SwiftSpatial)
Uniform Point-Polygon	9,212 ms	1,542 ms	305 ms
Uniform Polygon-Polygon	9,220 ms	2,061 ms	372 ms
OSM Point-Polygon	6,149 ms	881 ms	243 ms
OSM Polygon-Polygon	6,903 ms	13,779 ms	2,515 ms

4.8 Index Construction Cost

When interfaced with a spatial data management system, SwiftSpatial requires the R-trees to be constructed just once by the CPU during the system’s initialization phase. We study this one-time cost by implementing the index construction in C++ using the Sort-Tile-Recursive (STR) algorithm [38], which bulk loads the data to an R-tree using a recursive sorting and tiling strategy. We apply the parallel and vectorized sorting algorithm in the C++ Standard Template Library (STL). Table 2 compares the time spent constructing indexes versus executing the join operation (using C++ multi-thread and SwiftSpatial) on several datasets of ten million objects, adopting a max node size of 16 as it demonstrates optimal join performance on both CPUs and FPGAs. Since the construction cost is typically higher than the join itself, spatial join based on R-trees would benefit more from iterative spatial joins [64], where at least one dataset is dynamic. In such scenarios, the R-tree is constructed once at the beginning, and subsequent insertions, updates, or deletions result in only minimal indexing overhead compared to bulk loading. For one-off join, algorithms with less preprocessing overhead, such as PBSM, would be a better choice.

5 DISCUSSION

In this section, we discuss how SwiftSpatial can be adapted for deployments in real-world spatial data management systems.

Handling datasets larger than FPGA memory. So far, we have evaluated joins for which the indexed datasets and the join results fit in the FPGA memory. There are three potential solutions for larger-than-FPGA-memory joins. The first solution involves data partitioning, akin to big data frameworks. The data is partitioned, and the join operation is segmented into several sub-tasks, which are handled by multiple FPGAs before the results are aggregated. The second solution, given the significant speed advantage of FPGAs over software-based solutions, is that a single FPGA can process all data partitions iteratively. The third solution is to scale up the FPGA memory capacity: the FPGA, as a computational device on its own, can be equipped with an extended memory capacity, even up to a terabyte of memory per device [13].

Implementing alternative spatial join algorithms. While this paper uses R-tree synchronous traversal as SwiftSpatial’s control flow, SwiftSpatial’s modular design ensures its adaptability to other algorithms. This versatility stems from the reusability of the accelerator’s key component — the hardware join units — because joining small tiles is a major performance bottleneck in many spatial join algorithms [8, 47, 51, 68]. For instance, to implement PBSM’s control flow on SwiftSpatial, one only needs to adapt the on-chip scheduler to dispatch the same tile of the two datasets to the hardware join units in a round-robin fashion.

6 RELATED WORK

To the best of our knowledge, SwiftSpatial is the first specialized hardware architecture for spatial join. Since we have introduced the landscape of spatial join research in §2, we now shift our focus to discussing related work in the realm of spatial data management techniques and hardware acceleration for data processing.

Indexes for spatial data. The R-tree [27], introduced by Guttman in 1984, has been and continues to be one of the most popular index structures for managing spatial data. Various efforts have been undertaken to enhance the topology of the R-tree, aiming to speed up spatial queries. For instance, both STR [38] and the Hilbert R-tree [33] improve R-tree topologies by more effective bulk loading strategies. On the other hand, the R⁺ tree [57] and the R^{*} tree [6] focus on optimizing subtree selection for insertion and node splits, and recent advancements have incorporated reinforcement learning to guide those policies [26]. Apart from R-trees, there are other indexing techniques for spatial data. Quad-trees [55, 56], for instance, recursively divide space into four quadrants. Octrees [46] extend the quad-tree idea to three-dimensional spaces by recursively dividing the space into eight octants. KD-trees [49] split the space into two half-spaces along each of the k dimensions. BSP trees [23] use hyperplanes to recursively subdivide space into two convex sets. G-trees [40, 79] are optimized for improving query performance on road networks, a special type of spatial data.

Hardware acceleration for data management. As Moore’s Law has come to an end, substantial research has been devoted to processing data on hardware accelerators, among which GPUs and FPGAs have been the most popular options so far.

GPUs have been effectively utilized for a range of data management tasks including query processing [24, 29, 59], map-reduce functions [28], and graph traversals [41, 58]. While GPUs’ data processing performance can be limited by the PCIe bandwidth to the host server [24, 59], recent advancements in fast interconnect technologies between GPUs have enabled multiple accelerators to process analytical workloads collaboratively with the majority of data resided in the accelerator memory, thus minimizing data exchange with the host server [44, 52].

FPGAs have demonstrated potential not only in relational joins [9] but also in other database operations like regular expression matching queries [62], sketching [12, 35], and data partitioning [34]. Beyond these core database operations, FPGAs can accelerate graph traversal [10], high-dimensional approximate nearest neighbor search [32], data encryption and compression [11], etc.

7 CONCLUSION

We introduce SwiftSpatial, a hardware accelerator architecture for spatial join. It consists of specialized join units featuring hybrid parallelism, dedicated memory management units, and an on-chip scheduler that coordinates these components. Prototyped on FPGA, SwiftSpatial achieves a latency improvement of up to 5.36× compared to the best-performing software baseline, all while requiring 6.16× less power supply. The modular structure of SwiftSpatial enables (a) its flexible instantiation on both data-center-grade FPGAs and embedded systems and (b) its adaptability to various spatial join algorithms, indicating its extensive applicability in future spatial data management systems.

REFERENCES

- [1] [n.d.]. Apache Sedona. sedona.apache.org.
- [2] [n.d.]. AQUA (Advanced Query Accelerator) – A Speed Boost for Your Amazon Redshift Queries. <https://aws.amazon.com/blogs/aws/new-aqua-advanced-query-accelerator-for-amazon-redshift/>.
- [3] [n.d.]. cuSpatial. <https://github.com/rapidsai/cuspatial>.
- [4] [n.d.]. PostGIS. <http://postgis.net/>.
- [5] Ablimit Aji, Fusheng Wang, Hoang Vo, Rubao Lee, Qiaoling Liu, Xiaodong Zhang, and Joel Saltz. 2013. Hadoop gis: a high performance spatial data warehousing system over mapreduce. *Proceedings of the VLDB Endowment* 6, 11 (2013), 1009–1020.
- [6] Norbert Beckmann, Hans-Peter Kriegel, Ralf Schneider, and Bernhard Seeger. 1990. The R⁺-tree: An efficient and robust access method for points and rectangles. In *Proceedings of the 1990 ACM SIGMOD international conference on Management of data*. 322–331.
- [7] Thomas Brinkhoff, Hans-Peter Kriegel, Ralf Schneider, and Bernhard Seeger. 1994. Multi-step processing of spatial joins. *Acm Sigmod Record* 23, 2 (1994), 197–208.
- [8] Thomas Brinkhoff, Hans-Peter Kriegel, and Bernhard Seeger. 1993. Efficient processing of spatial joins using R-trees. *ACM SIGMOD Record* 22, 2 (1993), 237–246.
- [9] Xinyu Chen, Yao Chen, Ronak Bajaj, Jiong He, Bingsheng He, Weng-Fai Wong, and Deming Chen. 2020. Is FPGA useful for hash joins?. In *CIDR*.
- [10] Xinyu Chen, Hongshi Tan, Yao Chen, Bingsheng He, Weng-Fai Wong, and Deming Chen. 2021. ThunderGP: HLS-based graph processing framework on FPGAs. In *The 2021 ACM/SIGDA International Symposium on Field-Programmable Gate Arrays*. 69–80.
- [11] Monica Chiosa, Fabio Maschi, Ingo Müller, Gustavo Alonso, and Norman May. 2022. Hardware acceleration of compression and encryption in SAP HANA. In *48th International Conference on Very Large Databases (VLDB 2022)*.
- [12] Monica Chiosa, Thomas B Preußer, and Gustavo Alonso. 2021. Skt: A one-pass multi-sketch data analytics accelerator. *Proceedings of the VLDB Endowment* 14, 11 (2021), 2369–2382.
- [13] David Cock, Abishek Ramdas, Daniel Schwyn, Michael Giardino, Adam Turowski, Zhenhao He, Nora Hossle, Dario Korolija, Melissa Licciardello, Kristina Martsenko, et al. 2022. Enzian: an open, general, CPU/FPGA platform for systems software research. In *Proceedings of the 27th ACM International Conference on Architectural Support for Programming Languages and Operating Systems*. 434–451.
- [14] Mark De Berg, Marc Van Kreveld, Mark Overmars, Otfried Schwarzkopf, Mark de Berg, Marc van Kreveld, Mark Overmars, and Otfried Schwarzkopf. 1997. *Computational Geometry: Introduction*. Springer.
- [15] J-P Dittrich and Bernhard Seeger. 2000. Data redundancy and duplicate detection in spatial join processing. In *Proceedings of 16th International Conference on Data Engineering (Cat. No. 00CB37073)*. IEEE, 535–546.
- [16] Harish Doraiswamy and Juliana Freire. 2020. A gpu-friendly geometric data model and algebra for spatial queries. In *Proceedings of the 2020 ACM SIGMOD international conference on management of data*. 1875–1885.
- [17] Harish Doraiswamy and Juliana Freire. 2022. SPADE: GPU-Powered Spatial Database Engine for Commodity Hardware. In *2022 IEEE 38th International Conference on Data Engineering (ICDE)*. IEEE, 2669–2681.
- [18] Ahmed Eldawy, Louai Alarabi, and Mohamed F Mokbel. 2015. Spatial partitioning techniques in SpatialHadoop. *Proceedings of the VLDB Endowment* 8, 12 (2015), 1602–1605.
- [19] Ahmed Eldawy and Mohamed F Mokbel. 2015. The era of big spatial data. In *2015 31st IEEE International Conference on Data Engineering Workshops*. IEEE, 42–49.
- [20] Ahmed Eldawy and Mohamed F Mokbel. 2015. Spatialhadoop: A mapreduce framework for spatial data. In *2015 IEEE 31st international conference on Data Engineering*. IEEE, 1352–1363.
- [21] Yi Fang, Marc Friedman, Giri Nair, Michael Rys, and Ana-Elisa Schmid. 2008. Spatial indexing in microsoft SQL server 2008. In *Proceedings of the 2008 ACM SIGMOD international conference on Management of data*. 1207–1216.
- [22] Daniel Firestone, Andrew Putnam, Sambhrama Mundkur, Derek Chiou, Alireza Dabagh, Mike Andrewartha, Hari Angepat, Vivek Bhanu, Adrian Caulfield, Eric Chung, et al. 2018. Azure accelerated networking: Smartnets in the public cloud. In *15th {USENIX} Symposium on Networked Systems Design and Implementation ({NSDI} 18)*. 51–66.
- [23] Henry Fuchs, Zvi M Kedem, and Bruce F Naylor. 1980. On visible surface generation by a priori tree structures. In *Proceedings of the 7th annual conference on Computer graphics and interactive techniques*. 124–133.
- [24] Henning Funke, Sebastian Breß, Stefan Noll, Volker Markl, and Jens Teubner. 2018. Pipelined query processing in coprocessor environments. In *Proceedings of the 2018 International Conference on Management of Data*. 1603–1618.
- [25] Thanasis Georgiadis and Nikos Mamoulis. 2023. Raster Intervals: An Approximation Technique for Polygon Intersection Joins. *Proceedings of the ACM on Management of Data* 1, 1 (2023), 1–18.
- [26] Tu Gu, Kaiyu Feng, Gao Cong, Cheng Long, Zheng Wang, and Sheng Wang. 2023. The RLR-Tree: A Reinforcement Learning Based R-Tree for Spatial Data. *Proceedings of the ACM on Management of Data* 1, 1 (2023), 1–26.
- [27] Antonin Guttman. 1984. R-trees: A dynamic index structure for spatial searching. In *Proceedings of the 1984 ACM SIGMOD international conference on Management of data*. 47–57.
- [28] Bingsheng He, Wenbin Fang, Qiong Luo, Naga K Govindaraju, and Tuyong Wang. 2008. Mars: a MapReduce framework on graphics processors. In *Proceedings of the 17th international conference on Parallel architectures and compilation techniques*. 260–269.
- [29] Bingsheng He, Ke Yang, Rui Fang, Mian Lu, Naga Govindaraju, Qiong Luo, and Pedro Sander. 2008. Relational joins on graphics processors. In *Proceedings of the 2008 ACM SIGMOD international conference on Management of data*. 511–524.
- [30] Gui Huang, Xuntao Cheng, Jianying Wang, Yujie Wang, Dengcheng He, Tiejing Zhang, Feifei Li, Sheng Wang, Wei Cao, and Qiang Li. 2019. X-Engine: An optimized storage engine for large-scale E-commerce transaction processing. In *Proceedings of the 2019 International Conference on Management of Data*. 651–665.
- [31] Yun-Wu Huang, Ning Jing, Elke A Rundensteiner, et al. 1997. Spatial joins using R-trees: Breadth-first traversal with global optimizations. In *VLDB*, Vol. 97. 25–29.
- [32] Wenqi Jiang, Shigang Li, Yu Zhu, Johannes de Fine Licht, Zhenhao He, Runbin Shi, Cedric Renggli, Shuai Zhang, Theodoros Rekatsinas, Torsten Hoefler, et al. 2023. Co-design Hardware and Algorithm for Vector Search. *arXiv preprint arXiv:2306.11182* (2023).
- [33] Ibrahim Kamel and Christos Faloutsos. 1993. *Hilbert R-tree: An improved R-tree using fractals*. Technical Report.
- [34] Kaan Kara, Jana Giceva, and Gustavo Alonso. 2017. Fpga-based data partitioning. In *Proceedings of the 2017 ACM International Conference on Management of Data*. 433–445.
- [35] Martin Kiefer, Ilias Poulakis, Eleni Tzirita Zacharitou, and Volker Markl. 2023. Optimistic Data Parallelism for FPGA-Accelerated Sketching. *Proceedings of the VLDB Endowment* 16, 5 (2023), 1113–1125.
- [36] Ravi Kanth V Kothuri, Siva Ravada, and Daniel Abugov. 2002. Quadtree and R-tree indexes in oracle spatial: a comparison using GIS data. In *Proceedings of the 2002 ACM SIGMOD international conference on Management of data*. 546–557.
- [37] Hans-Peter Kriegel, Andreas Müller, Marco Pötke, and Thomas Seidl. 2001. Spatial data management for computer aided design. *ACM SIGMOD Record* 30, 2 (2001), 614.
- [38] Scott T Leutenegger, Mario A Lopez, and Jeffrey Edgington. 1997. STR: A simple and efficient algorithm for R-tree packing. In *Proceedings 13th international conference on data engineering*. IEEE, 497–506.
- [39] Feifei Li. 2019. Cloud-native database systems at Alibaba: Opportunities and challenges. *Proceedings of the VLDB Endowment* 12, 12 (2019), 2263–2272.
- [40] Zijian Li, Lei Chen, and Yue Wang. 2019. G-tree: An efficient spatial index on road networks. In *2019 IEEE 35th International Conference on Data Engineering (ICDE)*. IEEE, 268–279.
- [41] Hang Liu, H Howie Huang, and Yang Hu. 2016. ibfs: Concurrent breadth-first search on gpus. In *Proceedings of the 2016 International Conference on Management of Data*. 403–416.
- [42] Paul A Longley, Michael F Goodchild, David J Maguire, and David W Rhind. 2015. *Geographic information science and systems*. John Wiley & Sons.
- [43] Lijuan Luo, Martin DF Wong, and Lance Leong. 2012. Parallel implementation of R-trees on the GPU. In *17th Asia and South Pacific Design Automation Conference*. IEEE, 353–358.
- [44] Clemens Lutz, Sebastian Breß, Steffen Zeuch, Tilmann Rabl, and Volker Markl. 2020. Pump up the volume: Processing large data on GPUs with fast interconnects. In *Proceedings of the 2020 ACM SIGMOD International Conference on Management of Data*. 1633–1649.
- [45] Norman May, Daniel Ritter, Andre Dossinger, Christian Färber, and Suleyman Demirsoy. 2023. DASH: Asynchronous Hardware Data Processing Services. In *13th Conference on Innovative Data Systems Research, CIDR*.
- [46] Donald Meagher. 1982. Geometric modeling using octree encoding. *Computer graphics and image processing* 19, 2 (1982), 129–147.
- [47] Sadeq Nobari, Farhan Tauheed, Thomas Heinis, Panagiotis Karras, Stéphane Bressan, and Anastasia Ailamaki. 2013. TOUCH: in-memory spatial join by hierarchical data-oriented partitioning. In *Proceedings of the 2013 ACM SIGMOD International Conference on Management of Data*. 701–712.
- [48] Peter Ogden, David Thomas, and Peter Pietzuch. 2016. AT-GIS: highly parallel spatial query processing with associative transducers. In *Proceedings of the 2016 International Conference on Management of Data*. 1041–1054.
- [49] Jack A Orenstein and Tim H Merrett. 1984. A class of data structures for associative searching. In *Proceedings of the 3rd ACM SIGACT-SIGMOD Symposium on Principles of Database Systems*. 181–190.
- [50] Varun Pandey, Andreas Kipf, Thomas Neumann, and Alfons Kemper. 2018. How good are modern spatial analytics systems? *Proceedings of the VLDB Endowment* 11, 11 (2018), 1661–1673.
- [51] Jignesh M Patel and David J DeWitt. 1996. Partition based spatial-merge join. *ACM Sigmod Record* 25, 2 (1996), 259–270.

- [52] Johns Paul, Shengliang Lu, Bingsheng He, and Chiew Tong Lau. 2021. MG-Join: A scalable join for massively parallel multi-GPU architectures. In *Proceedings of the 2021 International Conference on Management of Data*. 1413–1425.
- [53] Sushil K Prasad, Michael McDermott, Xi He, and Satish Puri. 2015. GPU-based Parallel R-tree Construction and Querying. In *2015 IEEE International Parallel and Distributed Processing Symposium Workshop*. IEEE, 618–627.
- [54] Dale A Quattrochi and Michael F Goodchild. 1997. *Scale in remote sensing and GIS*. CRC press.
- [55] AndreasKipf HaraldLang VarunPandey RaulAlexandruPersa, Christoph Anneser Eleni Tzirita Zacharitou, Harish Doraiswamy, Peter Boncz, and Thomas Neumann Alfons Kemper. 2020. Adaptive Main-Memory Indexing for High-Performance Point-Polygon Joins. (2020).
- [56] Hanan Samet and Robert E Webber. 1985. Storing a collection of polygons using quadtrees. *ACM Transactions on Graphics (TOG)* 4, 3 (1985), 182–222.
- [57] Timos Sellis, Nick Roussopoulos, and Christos Faloutsos. 1987. The R+-Tree: A Dynamic Index for Multi-Dimensional Objects. (1987).
- [58] Mo Sha, Yuchen Li, and Kian-Lee Tan. 2019. Gpu-based graph traversal on compressed graphs. In *Proceedings of the 2019 International Conference on Management of Data*. 775–792.
- [59] Anil Shanbhag, Samuel Madden, and Xiangyao Yu. 2020. A study of the fundamental performance characteristics of GPUs and CPUs for database analytics. In *Proceedings of the 2020 ACM SIGMOD international conference on Management of data*. 1617–1632.
- [60] Darius Šidlauskas and Christian S Jensen. 2014. Spatial joins in main memory: Implementation matters! *Proceedings of the VLDB Endowment* 8, 1 (2014), 97–100.
- [61] Darius Šidlauskas, Simonas Šaltenis, Christian W Christiansen, Jan M Johansen, and Donatas Šaulys. 2009. Trees or grids? Indexing moving objects in main memory. In *Proceedings of the 17th ACM SIGSPATIAL international conference on Advances in Geographic Information Systems*. 236–245.
- [62] David Sidler, Zsolt István, Muhsen Owaida, and Gustavo Alonso. 2017. Accelerating pattern matching queries in hybrid CPU-FPGA architectures. In *Proceedings of the 2017 ACM International Conference on Management of Data*. 403–415.
- [63] Panagiotis Sioulas, Periklis Chrysogelos, Manos Karpathiotakis, Raja Apuswamy, and Anastasia Ailamaki. 2019. Hardware-conscious hash-joins on gpus. In *2019 IEEE 35th International Conference on Data Engineering (ICDE)*. IEEE, 698–709.
- [64] Benjamin Sowell, Marcos Vaz Salles, Tuan Cao, Alan Demers, and Johannes Gehrke. 2013. An experimental analysis of iterated spatial joins in main memory. *Proceedings of the VLDB Endowment* 6, 14 (2013), 1882–1893.
- [65] Chengyu Sun, Divyakant Agrawal, and Amr El Abbadi. 2003. Hardware acceleration for spatial selections and joins. In *Proceedings of the 2003 ACM SIGMOD international conference on Management of data*. 455–466.
- [66] Mingjie Tang, Yongyang Yu, Qutaibah M Malluhi, Mourad Ouzzani, and Walid G Aref. 2016. Locationspark: A distributed in-memory data management system for big spatial data. *Proceedings of the VLDB Endowment* 9, 13 (2016), 1565–1568.
- [67] Farhan Tauheed, Thomas Heinis, and Anastasia Ailamaki. 2015. THERMAL-JOIN: A scalable spatial join for dynamic workloads. In *Proceedings of the 2015 ACM SIGMOD International Conference on Management of Data*. 939–950.
- [68] Dimitrios Tsitsigkos, Panagiotis Bouros, Nikos Mamoulis, and Manolis Terrovitis. 2019. Parallel in-memory evaluation of spatial joins. In *Proceedings of the 27th ACM SIGSPATIAL International Conference on Advances in Geographic Information Systems*. 516–519.
- [69] Hoang Vo, Yanhui Liang, Jun Kong, and Fusheng Wang. 2018. iSPEED: a scalable and distributed in-memory based spatial query system for large and structurally complex 3D data. In *Proceedings of the VLDB Endowment. International Conference on Very Large Data Bases*, Vol. 11. NIH Public Access, 2078.
- [70] Dong Xie, Feifei Li, Bin Yao, Gefei Li, Liang Zhou, and Minyi Guo. 2016. Simba: Efficient in-memory spatial analytics. In *Proceedings of the 2016 international conference on management of data*. 1071–1085.
- [71] Simin You, Jianting Zhang, and Le Gruenwald. 2013. Parallel spatial query processing on gpus using r-trees. In *Proceedings of the 2Nd ACM SIGSPATIAL international workshop on analytics for big geospatial data*. 23–31.
- [72] Simin You, Jianting Zhang, and Le Gruenwald. 2015. Large-scale spatial join query processing in cloud. In *2015 31st IEEE international conference on data engineering workshops*. IEEE, 34–41.
- [73] Simin You, Jianting Zhang, and Le Gruenwald. 2015. Large-scale spatial join query processing in cloud. In *2015 31st IEEE international conference on data engineering workshops*. IEEE, 34–41.
- [74] Jia Yu, Jinxuan Wu, and Mohamed Sarwat. 2015. Geospark: A cluster computing framework for processing large-scale spatial data. In *Proceedings of the 23rd SIGSPATIAL international conference on advances in geographic information systems*. 1–4.
- [75] Eleni Tzirita Zacharitou, Harish Doraiswamy, Anastasia Ailamaki, Cláudio T Silva, and Juliana Freire. 2017. GPU rasterization for real-time spatial aggregation over arbitrary polygons. *Proceedings of the VLDB Endowment* 11, 3 (2017), 352–365.
- [76] Matei Zaharia, Mosharaf Chowdhury, Tathagata Das, Ankur Dave, Justin Ma, Murphy McCauly, Michael J Franklin, Scott Shenker, and Ion Stoica. 2012. Resilient distributed datasets: A {Fault-Tolerant} abstraction for {In-Memory} cluster computing. In *9th USENIX Symposium on Networked Systems Design and Implementation (NSDI 12)*. 15–28.
- [77] Teng Zhang, Jianying Wang, Xuntao Cheng, Hao Xu, Nanlong Yu, Gui Huang, Tieying Zhang, Dengcheng He, Feifei Li, Wei Cao, et al. 2020. FPGA-Accelerated Compactions for LSM-based Key-Value Store.. In *FAST*. 225–237.
- [78] Yu Zheng, Xing Xie, Wei-Ying Ma, et al. 2010. GeoLife: A collaborative social networking service among user, location and trajectory. *IEEE Data Eng. Bull.* 33, 2 (2010), 32–39.
- [79] Ruicheng Zhong, Guoliang Li, Kian-Lee Tan, Lizhu Zhou, and Zhiguo Gong. 2015. G-tree: An efficient and scalable index for spatial search on road networks. *IEEE Transactions on Knowledge and Data Engineering* 27, 8 (2015), 2175–2189.
- [80] Geraldo Zimbrão and Jano Moreira de Souza. 1998. A raster approximation for processing of spatial joins. In *VLDB*, Vol. 98. 24–27.